Journal Pre-proof

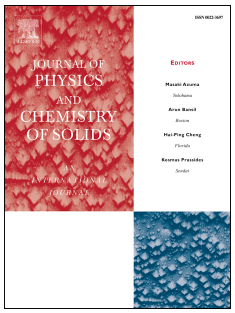

Sn-doped TiO_2 nanotubular thin film for photocatalytic degradation of methyl orange dye

Andjelika Bjelajac, Rada Petrović, Jelena Vujancevic, Katerina Veltruska, Vladimir Matolin, Zdravko Siketic, George Provatas, Milko Jaksic, George E. Stan, Gabriel Socol, Ion N. Mihailescu, Djordje Janaćković

PII: S0022-3697(19)32852-5

DOI: https://doi.org/10.1016/j.jpcs.2020.109609

Reference: PCS 109609

To appear in: *Journal of Physics and Chemistry of Solids*

Received Date: 24 December 2019

Revised Date: 2 June 2020

Accepted Date: 3 June 2020

Please cite this article as: A. Bjelajac, R. Petrović, J. Vujancevic, K. Veltruska, V. Matolin, Z. Siketic, G. Provatas, M. Jaksic, G.E. Stan, G. Socol, I.N. Mihailescu, D. Janaćković, Sn-doped TiO_2 nanotubular thin film for photocatalytic degradation of methyl orange dye, *Journal of Physics and Chemistry of Solids* (2020), doi: https://doi.org/10.1016/j.jpcs.2020.109609.

This is a PDF file of an article that has undergone enhancements after acceptance, such as the addition of a cover page and metadata, and formatting for readability, but it is not yet the definitive version of record. This version will undergo additional copyediting, typesetting and review before it is published in its final form, but we are providing this version to give early visibility of the article. Please note that, during the production process, errors may be discovered which could affect the content, and all legal disclaimers that apply to the journal pertain.

© 2020 Published by Elsevier Ltd.

Journal Pre-proof

Andjelika Bjelajac: Conceptualization, Formal analysis, Investigation, Writing - Original Draft, Visualization, Funding acquisition
Rada Petrović: Writing - Review & Editing, Supervision
Jelena Vujancevic: Formal analysis, Writing - Review & Editing, Visualization
Katerina Veltruska: Formal analysis, Investigation, Writing - Review & Editing
Vladimir Matolin: Data Curation, Funding acquisition
Zdravko Siketic: Formal analysis, Investigation, Writing - Review & Editing
George Provatas: Formal analysis, Investigation
Milko Jaksic: Data Curation, Funding acquisition
George E. Stan: Formal analysis, Investigation, Writing - Review & Editing
Gabriel Socol: Investigation, Formal analysis, Writing - Review & Editing
Ion N. Mihailescu: Writing - Review & Editing, Funding acquisition
Djordje Janaćković: Project administration, Funding acquisition

Journal Pre-proof

Journal Pre-proof

Sn-doped TiO_2 nanotubular thin film for photocatalytic degradation of methyl orange dye

Andjelika Bjelajac [a,*,1], Rada Petrović [b], Jelena Vujancevic [c], Katerina Veltruska [d], Vladimir Matolin [d], Zdravko Siketic [e], George Provatas [e], Milko Jaksic [e], George E. Stan [f], Gabriel Socol [g], Ion N. Mihailescu [g], Djordje Janaćković [b]

[a] University of Belgrade, Innovation center of Faculty of Technology and Metallurgy, Karnegijeva 4, 11000 Belgrade, Serbia
[b] University of Belgrade, Faculty of Technology and Metallurgy, Karnegijeva 4,11000 Belgrade, Serbia
[c] Institute of Technical Sciences of SASA, Knez Mihailova 35/IV, 11000 Belgrade, Serbia
[d] Charles University in Prague, Faculty of Mathematics and Physics, Department of Surface and Plasma Science, V Holešovičkách 2, 180 00 Prague 8, Czech Republic
[e] Ruđer Bošković Institute, Bijenička cesta 54, 10000 Zagreb, Croatia
[f] National Institute of Materials Physics, Laboratory of Multifunctional Materials and Structures, Atomistilor 405A, RO-077125 Magurele, Ilfov, Romania
[g] National Institute for Lasers, Plasma, and Radiation Physics, Lasers Department, "Laser-Surface-Plasma Interactions" Laboratory, RO-77125 Magurele, Ilfov, Romania

Journal Pre-proof

Abstract

We fabricated Sn-doped TiO_2 nanotubular film via annealing of anodized TiO_2 nanotubes grown on F-SnO_2 (FTO) glass. Annealing was carried out at 500 °C in ambient air. Anatase crystal structure was achieved with no change in nanotubular morphology in respect to as-anodized amorphous TiO_2 nanotubes. The X-ray photoelectron spectroscopy analysis revealed Sn on the surface of TiO_2 film, following the thermal treatment, probably caused by the diffusion from FTO glass. Depth profile examination of the film chemical composition was conducted by elastic recoil detection analysis, which showed that in addition to the diffusion of Sn from FTO, diffusion of Ti to FTO concurrently occurred. Thus, a higher concentration of Sn was found at the bottom of the tubes, while a lower concentration was present on the tubes' surface top. This explains the improved optical response revealed by a diffuse reflectance spectroscopy. The absorption enhancement demonstrated that Sn-doped TiO_2 film was efficient in the degradation of methyl orange dye under visible light.

[*]Corresponding author: andelika.bjelajac@polytechnique.edu (A. Bjelajac).
[1]Present address: LPICM, Ecole Polytechnique, CNRS, IP Paris, 91128 Palaiseau, France

Journal Pre-proof

Keywords: Thin films; Nanostructures; Photoelectron spectroscopy

1. Introduction

Titanium dioxide (TiO_2) is a semiconductor with numerous applications based upon its remarkable photoactivity [1–4]. It absorbs UV light and generates electron–hole pairs that can be useful for degradation of organic substances in polluted water systems [5,6]. Titanium dioxide is widely used since it is cheap, abundant and easy to process [7]. One approach to enhance its photocatalytic performance is nanostructuring of TiO_2, which provides high specific surface areas and an increased number of photoactive sites [7,8]. The widely used anodization technique for obtaining highly ordered TiO_2 nanotubes (NTs) [9] is superior to other methods, since it provides self-organization of the NTs that are perpendicular to the substrate which makes the exploitation of the material's high specific surface enhanced [10]. Other explored methods for synthesis of TiO_2 NTs, such as hydrothermal or solvothermal [11], result in a random orientation on the substrate. Moreover, specific synthesis requirements, such as high pressure, high temperature and long reaction time, make them disadvantageous compared to the anodization technique [12]. Differing to TiO_2 thin films obtained by anodization, any catalyst in powder form requires filtration of the system for removal of the photocatalyst. The major benefit of anodized TiO_2 NTs for photocatalytic applications is the orthogonal separation of charge carriers due to their 1D structure, meaning that electrons and holes are spatially separated within the tube wall. This means that electrons are collected in the wall center and transported to the back contact, while holes are driven to the wall–solution interface [13]. In this study, we explored the use of Ti thin film applied on a conductive substrate, such as F-SnO_2 (FTO) glass [14] for the fabrication of photocatalytic nanotubular TiO_2 thin film. Because as-synthetized NTs are amorphous, annealing (>300 °C) is required for conversion to crystalline structure [15]. Indeed, amorphous TiO_2 includes structural defects and exhibits poor photocatalytic activity. The TiO_2 has three main types of crystal structures: anatase, rutile and brookite [16]. Among them, anatase possesses the best photocatalytic property due to long electron lifetime [17]. When annealed at 400 °C for 2 h, the amorphous TiO_2 films are completely converted to nano-crystalline anatase phase. When increasing calcination temperature, photocatalytic activity rises due to the formation of anatase TiO_2 and improvement of its crystalline quality [18]. With further increase of calcination temperature from 600 to 800 °C, the photocatalytic activity rapidly decreases due to vanishing of the anatase phase, collapse of NT structures and decrease of active surface area [15].

In a previous study, we noted that the diffusion of Sn from FTO to TiO_2 can be promoted by annealing [19]. The aim of this work is to intensify this effect in order to obtain Sn-doped TiO_2 thin film that can then be used as an improved photocatalyst with respect to undoped TiO_2 [20]. It is well known that doping of TiO_2 leads to generation of

Journal Pre-proof

inter-band levels in energy gap of TiO_2 and/or band gap narrowing [21]. Herein, we investigated the nature of Sn incorporation using X-ray photoelectron spectroscopy (XPS) and surveyed the atomic content into the depth of the film using Time-of-Flight Elastic Recoil Detection Analysis (TOF-ERDA). Scanning electron microscopy (SEM) was used to monitor possible morphological changes due to the annealing. The phase composition of the film was investigated by grazing incident X-ray diffraction (GIXRD). The optical properties of the film before and after annealing were determined by measuring their diffuse reflectance spectra (DRS). The photocatalytic activity of the doped film was studied by assessing the degradation of methyl orange (MO) dye.

2. Experimental

Radio frequency magnetron sputtering (RF-MS) technique was employed for the deposition of pure titanium (Ti) thin films onto FTO glass (PI-KEM Ltd, 200 nm FTO film, 12–14 Ω/cm^2). A Ti target (Alfa Aesar GmbH) was used in experiments. Prior to deposition, the FTO substrates were successively cleaned by ultrasonication in acetone, ethanol and deionized water. After drying they were mechanically set inside the deposition chamber, at 40 mm from the target. Films were sputtered using a Cesar RF Power Generator equipped with a Dressler RMC-1 Matching Controller (13.56 MHz) deposition system with a magnetron cathode with a plasma ring of ~50 mm diameter. The sputtering chamber was first evacuated down to a residual pressure of $\sim 2 \times 10^{-4}$ Pa. Then pure argon was admitted into the reactor chamber at a constant gas flow rate of 5 sccm. The sputtering was carried out for 1 h at a working pressure and electrical power of 0.5 Pa and 60 W, respectively.

The anodization of the sputtered Ti films was performed in ethylene glycol containing 0.3 wt% ammonium fluoride and 2 wt.% water. A platinum plate served as a cathode. The electrodes were placed 20 mm apart and voltage was set at 60 V. The anodization was stopped when reaching the transparency of the films (~10 min), indicating that all Ti was oxidized. Next, the samples were well rinsed with water and left to dry in air for 24 h. Subsequently, the dried samples were annealed in air at 500 °C for 2 h.

Surface morphology of the samples was studied using a Tescan Mira X3 FESEM. Transmission electron microscopy (TEM) imaging was performed using an image corrected FEI TITAN TEM operating at 300 kV. For TEM analysis the surfaces of the samples were scratched with a diamond wire and fragments collected by dragging the carbon grid over the scratched surface. The DRS were recorded using a Shimadzu 2600 UV-Vis spectrophotometer with an integrating sphere attachment within wavelength range 300–800 nm.

Journal Pre-proof

The crystal structure of the samples was investigated by GIXRD using a Rigaku SmartLab 3 kW system with CuK_α radiation (λ = 1.5418 Å), operated at 40 kV and 40 mA at room temperature. The incidence angle was set at 0.25° (to maximize the signal originating from TiO_2 NT arrays), and the scattered intensity was scanned in the 2θ range of 20–50° with a step size of 0.04° and scan speed of 0.25°/min (dwell time of 9.6 s).

The XPS analyses were performed using a 1253.6-eV MgK_α beam source to check the overall chemical composition of the samples. The charging of spectra was corrected according to adventitious carbon with BE at 284.8 eV. The surface cleaning was done by applying 2 keV of Ar^+ ionic etching for 10 min. The XPS spectra were analyzed by fitting the Shirley-type function (i.e. non-linear background) and a sum of Voigt functions, using KolXPD software.

The elemental depth profiles of the films were determined using TOF-ERDA. Measurements were performed using a 23-MeV $^{127}I^{6+}$ beam, with 20° incidence angle toward the sample surface, and TOF-ERDA spectrometer positioned at 37.5° in regard to the beam direction. More details about the TOF-ERDA spectrometer (and analytical method) can be found in refs. [22,23]. Data analysis was carried using simulation code Potku [24] and Monte Carlo (MC) code CORTEO [25].

Photocatalysis was evaluated by following the degradation of MO dye (5 mg/L) by immersing the TiO_2–FTO photocatalyst in 10 mL of dye solution and illuminating the system with a solar simulator lamp, with the sample 100 mm away from the light source. The first 30 min was considered as the time required for reaching adsorption–desorption equilibrium because a prolonged period of darkness did not lead to any change in dye concentration. The sampling was done at different time intervals and the dye concentration was inferred by measuring the absorbance of the solution on a Shimadzu 1800 UV-Vis spectrophotometer. The influence of photolysis was also investigated by following the dye degradation upon illumination without the TiO_2 photocatalyst.

3. Results and discussion

Surface morphology changes due to annealing were studied by comparing the FESEM micrographs collected before and after the thermal treatment. A careful analysis of the images showed that the annealing did not affect the NT morphology. Thus, Fig. 1a–c presents the review of only the as-anodized TiO_2 NTs, as there were no changes due to annealing. The NTs were ~60 nm wide, ~30 nm thick and ~500 nm long. Some TEM and HRTEM micrographs of the annealed sample are also given in Fig. 1d–f in order to present more clearly the structure and crystallinity of NTs.

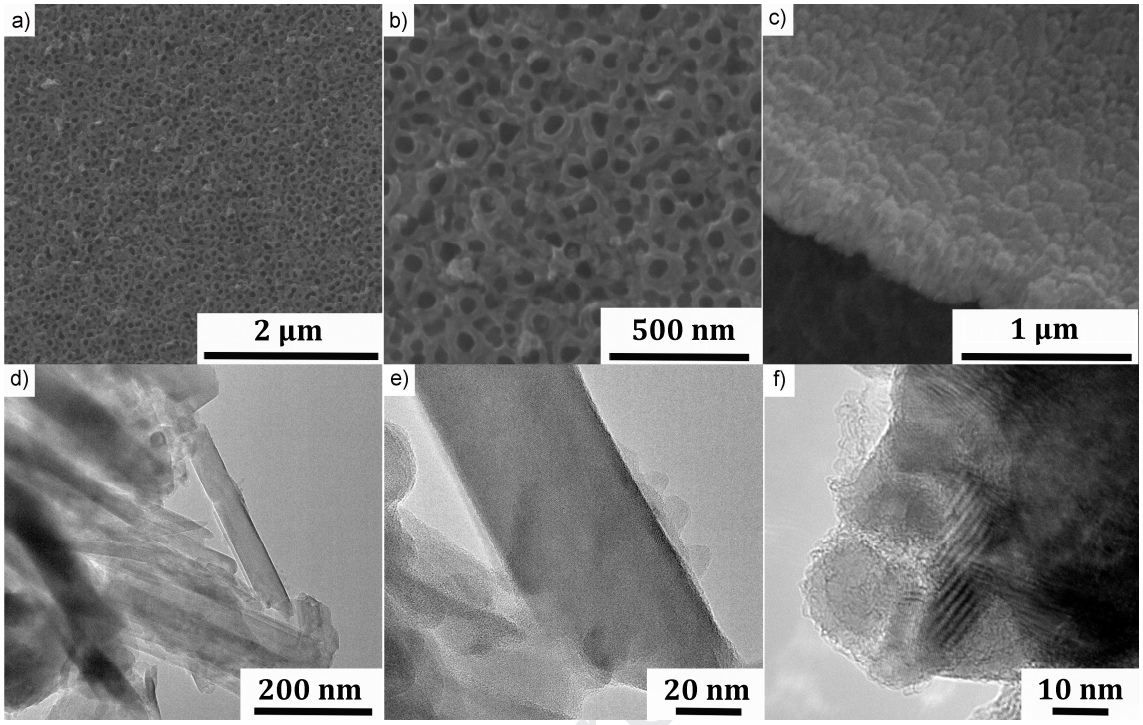

Fig. 1. FESEM and TEM micrographs of (a–c) as-anodized and (d–f) annealed TiO_2 nanotubes.

Phase composition of the annealed TiO_2–FTO sample vs. FTO substrate was investigated by GIXRD (Fig. 2). In addition to the diffraction maxima of the FTO substrate (a SnO_2-like phase, e.g. ICDD: 00-041-1445), the TiO_2 sample featured 101 and 200 reflections of anatase. The other anatase maxima (ICDD: 00-021-1272), peaking in this angular region, were superimposed by the higher intensity reflections of the substrate. Only the (103) crystal plane reflection was hinted by the slender shoulder appearing to the left-hand side of the prominent FTO substrate peak.

Crystalline coherence length ("crystallite size") was inferred from the full-width at half maximum of the 101 diffraction line of anatase, using the Scherrer equation [26]. The line width was corrected for instrumental broadening using a corundum standard reference (NIST SRM 1976). The crystallite size for 101 anatase reflection of annealed TiO_2 was ~45 nm.

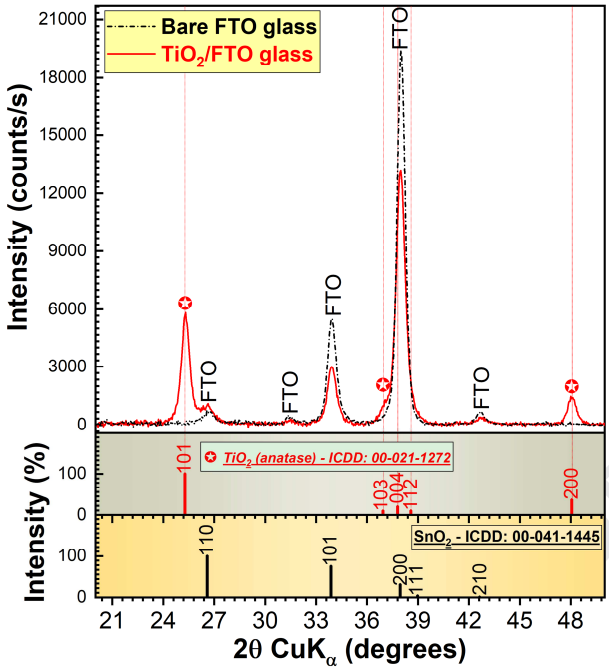

Fig. 2. Comparative GIXRD patterns of the bare FTO-glass substrate, and annealed TiO_2 film deposited onto FTO-glass substrate. For comparison, the ICDD: 00-021-1272 reference file of TiO_2-anatase is presented in the bottom graph together with ICDD: 00-041-1445 for SnO_2 phase.

In order to examine in more detail the annealing influence of TiO_2 film on FTO glass, the XPS analyses were performed on the amorphous and annealed TiO_2 films before Ar^+ ionic etching. The O 1s line was fitted and the results are presented in Fig. 3 together with Table 1 where the positions of the peaks are given.

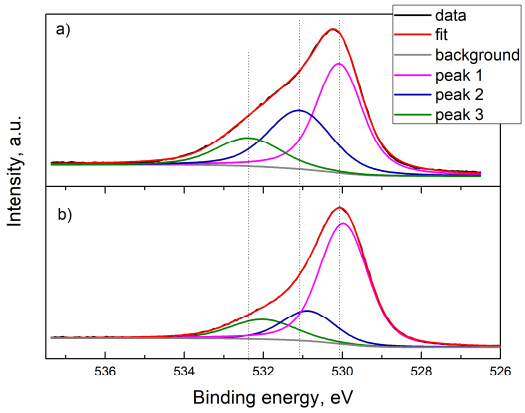

Fig. 3. XPS O 1s line for (a) amorphous and (b) annealed TiO_2 film, before Ar^+ ionic etching.

Peak 1 at ~530 eV was attributed to the lattice oxygen bound to Ti^{4+}, whereas peak 2 at ~531 eV corresponded to oxygen from surface OH groups [27] and bound to Ti^{3+} ions. Peak 3 at ~532 eV most probably originated from surface H_2O groups [27]. We cannot exclude, however, the contribution of oxygen bonded to C as a surface impurity. The

small shift of the peak 1 position to lower binding energy as a consequence of the annealing indicated a change in O environment. Moreover, the intensity of peak 2 decreased after annealing, which can mean that the amount of Ti^{3+} ions was diminished and consequently the number of oxygen vacancies decreased. This is supported by spectra of Ti 2p (Fig. 4). The presence of Ti^{3+} ions and oxygen vacancies is characteristic of nonstoichiometric TiO_2, with nonstoichiometry increasing as the amount of atmospheric oxygen decreased. After annealing in oxygen atmosphere, the nonstoichiometry decreased and so did the intensity of peak 2. The decrease of peak 2 intensity is also indicative of removal of OH groups on the surface.

Table 1 The position of O 1s line obtained by XPS analyses of TiO_2 films.

Sample	Position of peak 1 (eV)	Position of peak 2 (eV)	Position of peak 3 (eV)
Amorphous TiO_2	530.08	531.08	532.36
Annealed TiO_2 before Ar^+ ionic etching	529.97	530.86	532.01

After deconvolution of the Ti 2p line for the amorphous TiO_2 film (Fig. 4a), the four peaks were revealed: 464.39 eV ($2p_{1/2}$) and 458.66 eV ($2p_{3/2}$), which indicates the Ti^{4+} state; and 463.78 and 457.08 eV are associated with the Ti^{3+} state [27]. After annealing (Fig. 4b) the two peaks at 457.08 and 463.78 eV disappeared, demonstrating the decrease in oxygen vacancies. The two main peaks of the Ti^{4+} state did not change position (464.36 eV for $2p_{1/2}$ and 458.66 eV for $2p_{3/2}$).

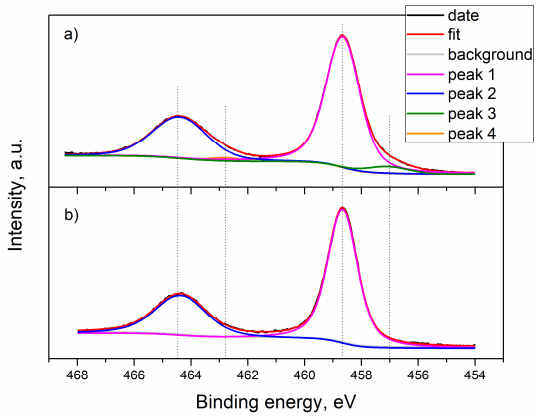

Fig. 4. XPS Ti 2p line for (a) amorphous and (b) annealed TiO_2 film, before Ar^+ ionic etching.

Chemical composition of the annealed TiO_2 film was assessed by XPS analysis. The compositional results obtained on the as-received sample (before Ar^+ ion etching) and after 10 min of Ar^+ ion etching are presented in Table 2. In both cases, Ti, O, Sn and C were detected. There was also a small amount of N in the case of the as-received sample. This could be N originating from surface weakly bonded species and would not affect the intrinsic properties of the material. The presence of C can also be attributed to

surface contaminants since its amount decreased from 18.15 to 9.45 at.% after Ar^+ ionic etching.

Table 2 Chemical composition of the annealed TiO_2 film determined by XPS before and after ionic etching.

Chemical composition (at.%)	O	C	Ti	Sn	N
Before Ar^+ ionic etching	58.05	18.15	22.26	0.15	1.40
After Ar^+ ionic etching	64.9	9.45	25.35	0.30	-

Presence of a certain quantity of Sn both before and after Ar^+ ionic etching should be emphasized. It is likely that Sn was incorporated in the TiO_2 lattice. Indeed, as already reported, at higher temperatures (>500 °C), Sn^{4+} from FTO glass diffuses into TiO_2 by substituting the Ti^{4+} ion [29]. To check this hypothesis, XPS analyses of Sn 3d core electron level were done (and compared) for the bare FTO-glass substrate and the annealed TiO_2 film–FTO glass (Fig. 5).

The Sn 3d line of FTO glass was fitted (Fig. 5a) as a doublet at 486.75 eV ($3d_{5/2}$) and 495.13 eV ($3d_{3/2}$), having the spin orbit separation of Δ = 8.38 eV, which is characteristic of Sn^{4+} in pure SnO_2 [30]. In the case of annealed TiO_2 film, these positions were slightly shifted to lower binding energies: 486.49 and 494.94 eV, and Δ = 8.45 eV (Fig. 5b). This means that Sn^{4+} was also present in the annealed TiO_2 film, since the positions of the characteristic peaks for Sn^{2+} were at significantly lower energies (484.7 eV for $3d_{5/2}$) [31]. It should be noted that for the as-anodized sample, the content of Sn was at the detection level limit, corresponding to 0.03 at.%, and peaks with BE of 486.83 and 495.32 eV were very close to those of FTO positions. The small shift of Sn $3d_{5/2}$ and $3d_{3/2}$ positions in annealed TiO_2 film to lower binding energies in regard to FTO glass can be accounted for by the increase of electron cloud density around Sn^{4+} ions due to higher electronegativity of Sn (1.96) vs. Ti (1.54). Indeed, the bigger the electron density around an ion is, the larger is the shift of binding energy positions toward lower energies. Particularly, Sn^{4+} ions in the TiO_2 structure attract electrons more than the Ti^{4+} ions do, leading to the shift of Sn $3d_{5/2}$ and $3d_{3/2}$ positions to lower binding energies compared to the position for pure SnO_2. Such shifts are indicative of a change in the surface electronic states, which ultimately can result in unique surface reactivity [32].

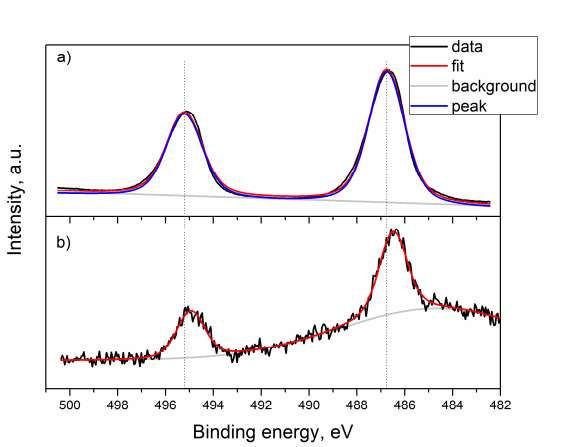

Fig. 5. XPS Sn 3d line for (a) FTO glass and (b) the annealed TiO_2 film, before Ar^+ ion etching

Because the XPS technique is only surface sensitive, depth profile composition was investigated by ToF-ERDA. The atomic contents of the elements of interest (Ti, O and Sn) showed an overlapping of the depth profiles for Sn and Ti in the range of 750–1300 at./cm^2 (Fig. 6). This indicates that potential diffusion of Sn from FTO occurred simultaneously with potential diffusion of Ti to FTO. Similar observations were previously reported for bilayer TiO_2–SnO_2 composite [29]. As expected, the Sn concentration was higher in the vicinity of SnO_2 film and gradually decreased toward the TiO_2 domain. The same trend was observed in the case of Ti diffusion to SnO_2. It was essential to combine XPS and ToF-ERDA methods to obtain a detailed insight concerning chemical composition of the sample. The XPS provided highly precise measurements of the surface, showing 0.15 at.% of Sn at the surface before ionic etching, whereas ToF-ERDA showed that the Sn concentration at the surface was 0 – thus the Sn concentration was much lower that the Ti and O concentrations, estimated as 33 and 67%, respectively.

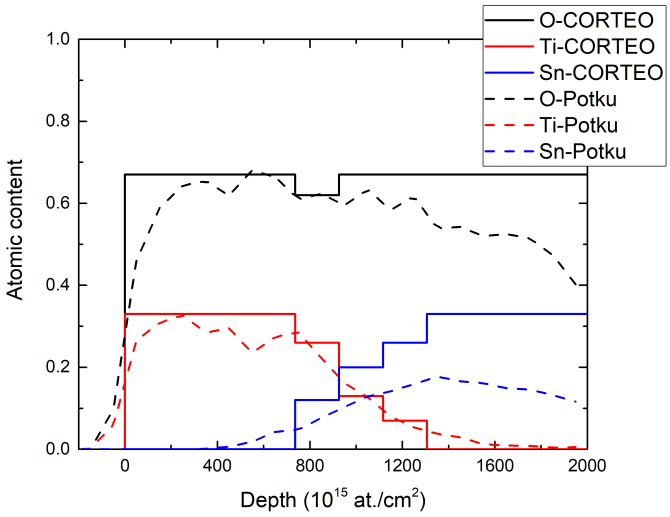

Journal Pre-proof

Fig. 6. Atomic content in depth of TiO_2 annealed film. Solid line-depth profile calculated by MC code CORTEO [22]. Dashed line-depth profile calculated using software Potku [21] (slab analysis).

It should be noted that the analyzed TiO_2 layer consisted of hollow NTs (non-homogeneous film, Fig. 1), while the depth scale in Fig. 6 represents only the average thickness of the TiO_2 film as "seen" by the ion beam probe. Depth profile steps in Fig. 6 are equal to 190×10^{15} at./cm^2, corresponding to ~20 nm (for the pure anatase TiO_2 with density of 4.23 g/cm^3). Furthermore, additional energy straggling of incoming and recoiled ions occurred, producing the broadening of measured energy spectra at the TiO_2–SnO_2 interface. Unfortunately, this extra contribution in energy straggling cannot be simulated even by MC code. Thus the depth profile in Fig. 6 is a convolution of diffusion between the layers and energy straggling through the non-homogeneous media.

In order to further investigate the effect of annealing on optical properties of the films, DRS spectra were recorded and compared (Fig. 7). The absorption edges were taken from the intersection of the tangent lines and a parallel to the x-axis that corresponded to the reflectance. The inferred values were λ = 413 and 425 nm for the as-anodized and annealed samples, respectively. The corresponding band gap energies, E_g, were calculated as hc/λ, where h is Planck's constant and c is the speed of light, and the E_g values were 3.0 and 2.92 eV for the as-anodized and annealed samples, respectively.

Because the characteristic absorption edge for anatase phase is 387 nm, we can deduce that in both cases there was a red shift of absorption. In the case of the non-calcinated sample, this could be due to N incorporation from NH_4F [33], but since the absorbance red shift was larger for the annealed sample, this was likely a consequence of Sn diffusion from FTO glass, as already evidenced by XPS analyses.

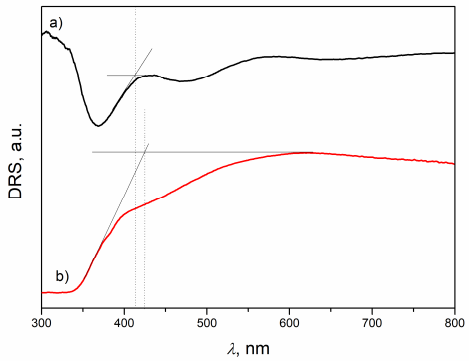

Fig. 7. DRS spectra of TiO_2 film (a) before and (b) after annealing.

The photocatalytic activity of TiO_2 films was studied by investigating the degradation of MO dye over time. No photocatalytic effect was recorded for the amorphous sample, even though a red shift of TiO_2 was observed. Most probably this was due to high recombination of the photoinduced charges, as expected in the case of amorphous

structures. We therefore present here only the results for the annealed TiO_2 (Fig. 8). The influence of photolysis was also investigated by monitoring the dye degradation upon illumination without the TiO_2 photocatalyst. Since there was no change in absorbance even after 6 h, the possibility of photolysis should be excluded (inset of Fig. 8a).

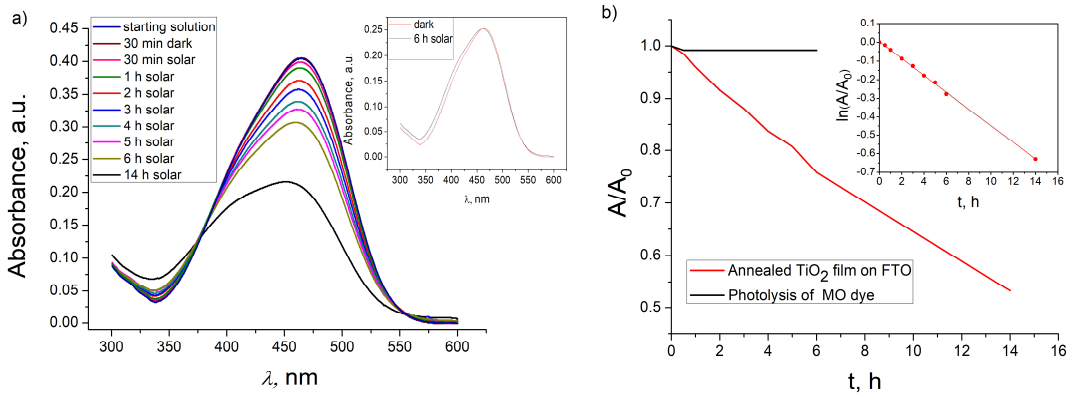

Fig. 8. (a) Absorbance spectra of methyl orange (MO) dye in the presence of annealed TiO_2 film upon solar illumination. Inset: results of MO photolysis in the absence of the catalyst during 6 h. (b) Efficiency of MO photodegradation as a function of time. Inset: linear transformation of photocatalytic data in order to determine *k*.

The absorption spectra of MO after visible light exposure is given in Fig. 8a, and the kinetic behavior of MO decomposition by the annealed TiO_2 film is shown in Fig. 8b. According to Fig. 8b and the straight line of function $\ln(A/A_o)$ on time *t*, it can be concluded that this photocatalytic reaction followed a pseudo-first order reaction:

$$\ln\left(\frac{A}{A_0}\right) = -kt \qquad (1).$$

where A_0 is initial absorbance of MO dye after adsorption–desorption equilibrium is reached, *A* is absorbance of dye at particular time *t* during the experiment and *k* is the pseudo-first order constant; *k* is calculated from the slope of the linear part and is 0.0453 h^{-1}. The reason for low value of *k* might be due to the clogging of the NTs with the gas molecules produced during the photodegradation of MO (CO_2 and H_2O) [34], since there was no stirring applied during the process. A well-designed agitated cell is necessary to further address this issue.

We believe that not only the extended absorption in the visible part favored the photocatalytic activity of the annealed TiO_2, but also that the charge recombination was reduced due to the TiO_2–SnO_2 interface. The presence of the TiO_2–SnO_2 interface is known to be beneficial for photocatalysis compared to the two-layered independent structure [29]. Photogenerated electrons are transferred from the conduction band of TiO_2 to that conduction band of SnO_2 which is lower than that of TiO_2. In other words, SnO_2 acts as a sink to collect electrons from TiO_2. On the other side, holes migrate in the opposite direction, from SnO_2 to TiO_2. This improves charge carrier separation and

Journal Pre-proof

reduces recombination [35]. Actually, Talinungsang et al. observed that the two-layer TiO_2–SnO_2–glass exhibited a higher degradation rate of methyl blue than just a monolayer deposited on a glass such as TiO_2–glass or SnO_2–glass [36]. Moreover, Cheng et al. [37] reported that the SnO_2–TiO_2 core-shell structure grown on indium doped tin oxide (ITO) glass had better photocatalytic performance than just the flat TiO_2 film deposited on ITO. The electron–hole pair separation was significantly improved for the SnO_2–TiO_2 core-shell structure due to the higher work function of SnO_2 than ITO. Duan et al. [38] investigated the influence of Sn content in TiO_2 photoanodes on efficiency of dye-sensitized solar cells. They showed that the electron lifetime and transport time decreased with increasing Sn/Ti ratio because electron density rose and increased the rate of recombination. Additionally, according to Liqian et al. [39], doping of TiO_2 with an appropriate amount of Sn enhanced photocatalytic activity compared to pure TiO_2. This is due to easier electron transfer from TiO_2 to SnO_2 due to the potential difference in conduction bands and so improves electron–hole separation. In addition to the valence band of SnO_2 being lower than for TiO_2, SnO_2 has a higher oxidation capability of photoinduced holes than TiO_2. Doping TiO_2 with Sn increases the ability of surface states on TiO_2 nanoparticles to bind photoinduced carriers to form more excitons.

This dynamic diffusion of Sn from FTO to the oxide top layer at high annealing temperature (500–550 °C) was also reported for hematite photoanodes. Shinde et al. [40] showed that diffusion of Sn was only in the direction of the hematite layer and not toward the glass support. Additionally, the FTO conductivity was preserved. Hence, we assumed that the diffusion of Sn occurred with the rearrangement of the Ti and O atoms during the transformation from amorphous to crystalline structure.

Based upon the measured dimensions of obtained NTs, we estimated that the porosity of the film was ~32 %, calculated using the equation for close packed tubes, as in our case [41]:

$$P = 1 - \frac{2\pi w(w + D)}{\sqrt{3}(D + 2w)^2} \qquad (2)$$

where D is the NT's inner diameter (60 nm) and w is the wall thickness (30 nm), as seen in Fig. 1. Taking into account the thickness of the film (~500 nm) and the 10 mm × 10 mm film surface, that would lead to 5×10^{-5} cm^3 × (1 − P) = 3.4×10^{-5} cm^3 for the volume of TiO_2. As the density of anatase is known to be 3.8 mg/cm^3, the amount of photocatalyst used was estimated as ~129 μg and the photocatalyst concentration was 13 μg/L. This information was used to compare the photocatalytic activity of the sample with previously published reports. However, direct comparison was difficult since this is the first study about TiO_2 NTs grown on FTO support that were shown to be doped with Sn by annealing. Studies of TiO_2 NTs grown on Ti support have reported longer and wider NTs with higher kinetic constant for degradation of MO, but also had different dye concentrations [42]. Some studies have presented the benefit of either P-

doping of TiO_2 anodized NTs on Ti foil [43] or coupling with Au nanoparticles [44] or even applying an external bias [45]. Another study of Sn-doped TiO_2 fibers synthesized by electrospinning reported almost complete MO degradation under visible light after 150 min but the concentration of the catalyst was much higher (400 mg/L) and the catalyst was dispersed as a powder in 20 ppm MO solution [46]. A direct comparison with our results is therefore quite difficult.

One of the methods to improve the photocatalytic activity of such a system as this, without embedding in heterostructures (e.g. ZnO–Au–TiO_2 [47]), would be Ar/O_2 plasma treatment, which increases the hydrophilicity of the TiO_2 films [48]. Apart from plasma treatment, annealing in different atmospheres, such as NH_3, is another way to dope TiO_2 with N and enhance the absorption properties of the film [49].

4. Conclusion

The TiO_2 NT films were fabricated by anodization of a Ti film sputtered on FTO glass. The XPS analyses were performed to study the chemical composition of the film before and after annealing in air at 500 °C. The annealing caused the simultaneous diffusion of Sn into TiO_2 film as well as Ti diffusion to the SnO_2 supporting film. By fitting the O 1s line, a small shift to lower binding energy was observed. This indicated a modification of the chemical environment of O due to Sn diffusion and conversion from an amorphous to a crystal structure. The XPS analysis showed that even at the surface of TiO_2 there was 0.10 at.% of Sn before and 0.30 at.% after ionic etching, and the ToF-ERDA investigations revealed a potential gradual increase of Sn concentration toward the bottom of the NTs. The DRS measurements showed that the annealing induced the absorption red shift from 413 to 425 nm and consequently a positive photocatalytic effect for the degradation of MO dye. Obviously, the presence of the TiO_2–SnO_2 interface was beneficial for photocatalysis. We believe that not only the extended absorption in the visible part favored photocatalytic activity of the annealed TiO_2, but also that the recombination of charges was reduced due to the TiO_2–SnO_2 interface and the appropriate energy level arrangements. This study indicates that TiO_2–SnO_2 coupling is a promising direction for further research in the field of photocatalysts based on TiO_2 NTs.

Acknowledgments

The Serbian authors acknowledge with thanks the financial support of the Ministry of Education, Science and Technological Development, Republic of Serbia (Projects III 45019 and Contracts No. 451-03-68/2020-14/200287 and 451-03-68/2020-14/200135).

The XPS and ToF-ERDA analyses were accomplished thanks to the financial support of the CERIC-ERIC (20177018 proposal) and Structure Fund Project CZ.02.1.01/0.0/0.0/16_013/0001788. The INFLPR authors acknowledge with thanks the partial financial support of this work by UEFISCDI under the contract ID 304/2011. GES thanks the NIMP Core Programme 21N.

References

[1] A. Fujishima, T.N. Rao, D.A. Tryk, Titanium dioxide photocatalysis, J. Photochem. Photobiol. C Photochem. Rev. 1 (2000) 1–21. https://doi.org/10.1016/S1389-5567(00)00002-2.

[2] K. Hashimoto, H. Irie, A. Fujishima, TiO_2 photocatalysis: a historical overview and future prospects, Jpn. J. Appl. Phys. 44 (2005) 8269–8285. https://doi.org/10.1143/JJAP.44.8269.

[3] V. Etacheri, C. Di Valentin, J. Schneider, D. Bahnemann, S.C. Pillai, Visible-light activation of TiO_2 photocatalysts: advances in theory and experiments, J. Photochem. Photobiol. C Photochem. Rev. 25 (2015) 1–29. https://doi.org/10.1016/j.jphotochemrev.2015.08.003.

[4] P. Górska, A. Zaleska, E. Kowalska, T. Klimczuk, J.W. Sobczak, E. Skwarek, W. Janusz, J. Hupka, TiO_2 photoactivity in vis and UV light: the influence of calcination temperature and surface properties, Appl. Catal. B Environ. 84 (2008) 440–447. https://doi.org/10.1016/j.apcatb.2008.04.028.

[5] Y. Kuwahara, J. Aoyama, K. Miyakubo, T. Eguchi, T. Kamegawa, K. Mori, H. Yamashita, TiO_2 photocatalyst for degradation of organic compounds in water and air supported on highly hydrophobic FAU zeolite: structural, sorptive, and photocatalytic studies, J. Catal. 285 (2012) 223–234. https://doi.org/10.1016/j.jcat.2011.09.031.

[6] S. Javed, M. Islam, M. Mujahid, Synthesis and characterization of TiO_2 quantum dots by sol gel reflux condensation method, Ceram. Int. 45 (2019) 2676–2679. https://doi.org/10.1016/j.ceramint.2018.10.163.

[7] S.M. Gupta, M. Tripathi, A review of TiO_2 nanoparticles, Chinese Sci. Bull. 56 (2011) 1639–1657. https://doi.org/10.1007/s11434-011-4476-1.

[8] H. Lin, C.P. Huang, W. Li, C. Ni, S.I. Shah, Y.H. Tseng, Size dependency of nanocrystalline TiO_2 on its optical property and photocatalytic reactivity exemplified by 2-chlorophenol, Appl. Catal. B Environ. 68 (2006) 1–11. https://doi.org/10.1016/j.apcatb.2006.07.018.

[9] Q. Pang, L. Leng, L. Zhao, L. Zhou, C. Liang, Y. Lan, Dye sensitized solar cells using freestanding TiO_2 nanotube arrays on FTO substrate as photoanode, Mater. Chem. Phys. 125 (2011) 612–616. https://doi.org/10.1016/j.matchemphys.2010.10.009.

[10] A. Bjelajac, V. Djokić, R. Petrović, N. Bundaleski, G. Socol, I.N. Mihailescu, Z. Rakočević, Dj. Janaćković, Absorption boost of TiO_2 nanotubes by doping with N and sensitization with CdS quantum dots, Ceram. Int. 43 (2017) 15040–15046. https://doi.org/10.1016/j.ceramint.2017.08.029.

[11] Y. Okour, H.K. Shon, I.J. El Saliby, R. Naidu, J.B. Kim, J.H. Kim, Preparation and characterisation of titanium dioxide (TiO_2) and thiourea-doped titanate

nanotubes prepared from wastewater flocculated sludge, Bioresour. Technol. 101 (2010) 1453–1458. https://doi.org/10.1016/j.biortech.2009.06.096.

[12] Y. Suzuki, S. Yoshikawa, Synthesis and thermal analyses of TiO_2-derived nanotubes prepared by the hydrothermal method, J. Mater. Res. 19 (2004) 982–985. https://doi.org/10.1557/JMR.2004.0128.

[13] X. Zhou, N. Liu, P. Schmuki, Photocatalysis with TiO_2 nanotubes: "Colorful" reactivity and designing site-specific photocatalytic centers into TiO_2 nanotubes, ACS Catal. 7 (2017) 3210–3235. https://doi.org/10.1021/acscatal.6b03709.

[14] Y.X. Tang, J. Tao, Y.Y. Zhang, T. Wu, H.J. Tao, Y.R. Zhu, Preparation of TiO_2 nanotube on glass by anodization of Ti films at room temperature, Trans. Nonferrous Met. Soc. China (English Ed.) 19 (2009) 192–198. https://doi.org/10.1016/S1003-6326(08)60251-4.

[15] G. Li, Z.-Q. Liu, J. Lu, L. Wang, Z. Zhang, Effect of calcination temperature on the morphology and surface properties of TiO_2 nanotube arrays, Appl. Surf. Sci. 255 (2009) 7323–7328. https://doi.org/10.1016/j.apsusc.2009.03.097.

[16] R. Khan, S. Javed, M. Islam, Hierarchical nanostructures of titanium dioxide: synthesis and applications, in: D. Yang (Ed), Titanium Dioxide - Material for a Sustainable Environment, IntechOpen, 2018, pp. 1–40. doi:10.5772/intechopen.74525.

[17] J. Wang, Q. Cai, H. Li, Y. Cui, H. Wang, A review on TiO_2 nanotube film photocatalysts prepared by liquid-phase deposition, Int. J. Photoenergy. 2012 (2012) 702940. https://doi.org/10.1155/2012/702940.

[18] S. Sreekantan, K.A. Saharudin, L.C. Wei, Formation of TiO_2 nanotubes via anodization and potential applications for photocatalysts, biomedical materials, and photoelectrochemical cell, IOP Conf. Ser. Mater. Sci. Eng. 21 (2011) 012002. https://doi.org/10.1088/1757-899X/21/1/012002.

[19] A. Bjelajac, R. Petrović, V. Djokic, V. Matolin, M. Vondraček, K. Dembele, S. Moldovan, O. Ersen, G. Socol, I.N. Mihailescu, Dj. Janaćković, Enhanced absorption of TiO_2 nanotubes by N-doping and CdS quantum dots sensitization: Insight into the structure, RSC Adv. 8 (2018) 35073–35082. https://doi.org/10.1039/c8ra06341a.

[20] A. Zaleska, Doped-TiO_2: a review, Recent Patents Eng. 2 (2008) 157–164. https://doi.org/10.2174/187221208786306289.

[21] M.K. Tariq, A. Riaz, R. Khan, A. Wajid, H.U. Haq, S. Javed, M.A. Akram, M. Islam, Comparative study of Ag, Sn or Zn doped TiO_2 thin films for photocatalytic degradation of methylene blue and methyl orange, Mater. Res. Express. 6 (2019) 106435. https://doi.org/10.1088/2053-1591/ab3efd.

[22] Z. Siketić, I.B. Radović, M. Jakšić, Development of a time-of-flight spectrometer at the Ruder Bošković Institute in Zagreb, Nucl. Instruments Methods Phys. Res. Sect. B Beam Interact. with Mater. Atoms. 266 (2008) 1328–1332. https://doi.org/10.1016/j.nimb.2007.12.070.

[23] Z. Siketić, I.B. Radović, M. Jakšić, Quantitative analysis of hydrogen in thin films using Time-of-Flight Elastic Recoil Detection Analysis, Thin Solid Films 518 (2010) 2617–2622. https://doi.org/10.1016/j.tsf.2009.07.196.

[24] K. Arstila, J. Julin, M.I. Laitinen, J. Aalto, T. Konu, S. Karkkainen, S. Rahkonen, M. Raunio, J. Itkonen, J.-P. Santanen, T. Tuovinen, T. Sajavaara, Potku-new analysis software for heavy ion elastic recoil detection analysis, Nucl. Instr. Meth. B. 331 (2014) 34–41. https://doi.org/10.1016/j.nimb.2014.02.016

[25] F. Schiettekatte, Fast Monte Carlo for ion beam analysis simulations, Nucl. Instr. Meth. B. 266 (2008) 1880. https://doi.org/10.1016/j.nimb.2007.11.075
[26] A.L. Patterson, The Scherrer formula for X-ray particle size determination, Phys. Rev. 56 (1939) 978–982. https://doi.org/10.1103/PhysRev.56.978.
[27] M.J. Jackman, A.G. Thomas, C. Muryn, Photoelectron spectroscopy study of stoichiometric and reduced anatase TiO_2 (101) surfaces: The effect of subsurface defects on water adsorption at near-ambient pressures, J. Phys. Chem. C. 119 (2015) 13682–13690. https://doi.org/10.1021/acs.jpcc.5b02732.
[28] B. Santara, P.K. Giri, K. Imakita, M. Fujii, Evidence of oxygen vacancy induced room temperature ferromagnetism in solvothermally synthesized undoped TiO_2 nanoribbons, Nanoscale 5 (2013) 5476–5488. https://doi.org/10.1039/c3nr00799e.
[29] J. Shang, W. Yao, Y. Zhu, N. Wu, Structure and photocatalytic performances of glass/SnO_2/TiO_2 interface composite film, Appl. Catal. A. Gen. 257 (2004) 25–32. https://doi.org/10.1016/j.apcata.2003.07.001.
[30] S.G. Ansari, M.A. Dar, M.S. Dhage, Y.S. Kim, Z.A. Ansari, A. Al-Hajry, H.S. Shin, A novel method for preparing stoichiometric SnO_2 thin films at low temperature, Rev. Sci. Instrum. 80 (2009). https://doi.org/10.1063/1.3115222.
[31] D. Toloman, O. Pana, M. Stefan, A. Popa, C. Leostean, S. Macavei, D. Silipas, I. Perhaita, M.D. Lazar, L. Barbu-Tudoran, Photocatalytic activity of SnO_2-TiO_2 composite nanoparticles modified with PVP, J. Colloid Interface Sci. 542 (2019) 296–307. https://doi.org/10.1016/j.jcis.2019.02.026.
[32] L. Xu, E.M.P. Steinmiller, S.E. Skrabalak, Achieving synergy with a potential photocatalytic Z-scheme: Synthesis and evaluation of nitrogen-doped TiO_2/SnO_2 composites, J. Phys. Chem. C. 116 (2012) 871–877. https://doi.org/10.1021/jp208981h.
[33] L. Lei, Y. Su, M. Zhou, X. Zhang, X. Chen, Fabrication of multi-non-metal-doped TiO_2 nanotubes by anodization in mixed acid electrolyte, Mater. Res. Bull. 42 (2007) 2230–2236. https://doi.org/10.1016/j.materresbull.2007.01.001.
[34] A.O. Ibhadon, P. Fitzpatrick, Heterogeneous photocatalysis: Recent advances and applications, Catalysts. 3 (2013) 189–218. https://doi.org/10.3390/catal3010189.
[35] M. Shipochka, A. Eliyas, I. Stambolova, V. Blaskov, S. Vassilev, S. Simeonova, K. Balashev, Synthesis of TiO_2 on SnO_2 bicomponent system and investigation of its structure and photocatalytic activity, Mater. Chem. Phys. 220 (2018) 249–259. https://doi.org/10.1016/j.matchemphys.2018.08.054.
[36] Talinungsang, N. Paul, D.D. Purkayastha, M.G. Krishna, TiO_2/SnO_2 and SnO_2/TiO_2 heterostructures as photocatalysts for degradation of stearic acid and methylene blue under UV irradiation, Superlattices Microstruct. 129 (2019) 105–114. https://doi.org/10.1016/j.spmi.2019.03.004.
[37] H.-E. Cheng, C.-Y. Lin, C.-M. Hsu, Fabrication of SnO_2-TiO_2 core-shell nanopillar-array films for enhanced photocatalytic activity, Appl. Surf. Sci. 396 (2017) 393–399. https://doi.org/10.1016/j.apsusc.2016.10.166.
[38] Y. Duan, N. Fu, Q. Liu, Y. Fang, X. Zhou, J. Zhang, Y. Lin, Sn-doped TiO_2 photoanode for dye-sensitized solar cells, J. Phys. Chem. C. 116 (2012) 8888–8893. https://doi.org/10.1021/jp212517k.
[39] J. Liqiang, F. Honggang, W. Baiqi, W. Dejun, X. Baifu, L. Shudan, S. Jiazhong, Effects of Sn dopant on the photoinduced charge property and photocatalytic activity of TiO_2 nanoparticles, Appl. Catal. B Environ. 62 (2006) 282–291.

https://doi.org/10.1016/j.apcatb.2005.08.012.
[40] P.S. Shinde, A. Annamalai, J.H. Kim, S.H. Choi, J.S. Lee, J.S. Jang, Exploiting the dynamic Sn diffusion from deformation of FTO to boost the photocurrent performance of hematite photoanodes, Sol. Energy Mater. Sol. Cells. 141 (2015) 71–79. https://doi.org/10.1016/j.solmat.2015.05.020.
[41] P. Quitério, A. Apolinário, C.T. Sousa, J.D. Costa, J. Ventura, J.P. Araújo, The cyclic nature of porosity in anodic TiO_2 nanotube arrays, J. Mater. Chem. A. 3 (2015) 3692–3698. https://doi.org/10.1039/C4TA04607B.
[42] Y.R. Smith, A. Kar, V.R. Subramanian, Investigation of physicochemical parameters that influence photocatalytic degradation of methyl orange over TiO_2 nanotubes, Ind. Eng. Chem. Res. 48 (2009) 10268–10276. https://doi.org/10.1021/ie801851p
[43] K.A. Saharudin, S. Sreekantan, P-incorporated TiO_2 nanotubes for methyl orange degradation, Adv. Mater. Res. 620 (2013) 151–155. https://doi.org/10.4028/www.scientific.net/AMR.620.151.
[44] C. Fu, M. Li, H. Li, C. Li, X. G. Wu, B. Yang, Fabrication of Au nanoparticle/TiO_2 hybrid films for photoelectrocatalytic degradation of methyl orange, J. Alloys Compd. 692 (2017) 727–733. https://doi.org/10.1016/j.jallcom.2016.09.119.
[45] Y.S. Sohn, Y.R. Smith, M. Misra, V.R. Subramanian, Electrochemically assisted photocatalytic degradation of methyl orange using anodized titanium dioxide nanotubes, Appl. Catal. B Environ. 84 (2008) 372–378. https://doi.org/10.1016/j.apcatb.2008.04.021.
[46] A.K. Alves, F.A. Berutti, C.P. Bergmann, Visible and UV photocatalytic characterization of Sn-TiO_2 electrospun fibers, Catal. Today. 208 (2013) 7–10. https://doi.org/10.1016/j.cattod.2012.10.020.
[47] F. Javed, S. Javed, M.A. Akram, M. Mujahid, M. Islam, A.S. Bhatti, Surface plasmon mediated optical properties of ZnO/Au/TiO_2 nanoheterostructure rod arrays, Mater. Sci. Eng. B Solid-State Mater. Adv. Technol. 231 (2018) 32–39. https://doi.org/10.1016/j.mseb.2018.08.001.
[48] A. Achour, M. Islam, S. Solaymani, S. Vizireanu, K. Saeed, G. Dinescu, Influence of plasma functionalization treatment and gold nanoparticles on surface chemistry and wettability of reactive-sputtered TiO_2 thin films, Appl. Surf. Sci. 458 (2018) 678–685. https://doi.org/10.1016/j.apsusc.2018.07.145.
[49] A. Bjelajac, R. Petrović, M. Popović, Z. Rakočević, G. Socol, I.N. Mihailescu, Dj. Janaćković, Doping of TiO_2 nanotubes with nitrogen by annealing in ammonia for visible light activation: Influence of pre- and post-annealing in air, Thin Solid Films. 692 (2019). https://doi.org/10.1016/j.tsf.2019.137598.

Journal Pre-proof

Journal Pre-proof

- Nanotubular TiO_2 film was obtained by anodization of Ti sputtered on F-SnO_2 glass.
- XRD showed that annealing in air at 500 °C resulted in anatase phase of TiO_2.
- XPS and ToF-ERDA were used to investigate possible Sn diffusion from F-SnO_2.
- Sn-doping of TiO_2 could be the reason for improved absorbance shifting to 425 nm.
- Sn-doped TiO_2 film was shown effective in the degradation of methyl orange dye.

Journal Pre-proof

Journal Pre-proof

Declaration of interests

☒ The authors declare that they have no known competing financial interests or personal relationships that could have appeared to influence the work reported in this paper.

Journal Pre-proof